ALL-OPTICAL ION BEAM COOLING AND ONLINE DIAGNOSTICS AT RELATIVISTIC ENERGIES

M. Bussmann[*], U.Schramm, Forschungszentrum Dresden-Rossendorf, D-01328 Dresden
W. Nörtershäuser, C. Novotny, C. Geppert, Johannes-Gutenberg-Universität Mainz, D-55099 Mainz
Th. Walther, G. Birkl, Technische Universität Darmstadt, D-64289 Darmstadt
D.F.A. Winters[a], Th. Kühl, C. Kozhuharov, M. Steck, F. Nolden, C. Dimopoulou, Th. Stöhlker[a]
GSI Helmholtzzentrum für Schwerionenforschung GmbH, D-64291 Darmstadt
[a] Ruprecht-Karls-Universität Heidelberg, D-69120 Heidelberg

Abstract

Recent experiments [1, 2] at the Experimental Storage Ring (ESR) at GSI have shown that relativistic Li-like C^{3+} ion beams can be cooled to an unprecedented momentum spread of $\Delta p/p \approx 10^{-7}$ using a single-frequency laser tuned to the Doppler-shifted $2S_{1/2} \rightarrow 2P_{1/2}$ and $2S_{1/2} \rightarrow 2P_{3/2}$ atomic transitions.

Although these results encourage the application of laser cooling to beams of other Li-like and Na-like ions at even higher energies as will be available at future storage rings at FAIR (Facility for Antiproton and Ion Research), two major concepts have to be demonstrated experimentally: First, efficient laser cooling of ion beams with large initial momentum spread, thus avoiding additional electron cooling to match the large momentum spread to the usually small momentum acceptance of the laser force. Second, all-optical measurements of the relevant beam parameters, thus overcoming the limited resolution of standard storage ring detectors such as the Schottky pickup electrode at ultra-low momentum spreads. The aim of this paper is to discuss the technical realization of these concepts as planned for an upcoming beam time at ESR.

PROSPECTS OF LASER COOLING ION BEAMS AT RELATIVISTIC ENERGIES

Future ion storage ring facilities such as FAIR will provide access to ultra-high energy beams of stable and rare ions for fundamental research. Many of the experiments planned at these facilities, such as in-ring mass spectrometry of short-lived rare nuclei, tests of strong-field quantum electrodynamics with highly-charged ions or in-beam x-ray spectroscopy of atomic transitions in heavy nuclei will greatly benefit from ion beams with ultra-low momentum spread. When considering relativistic ions at energies of several hundred MeV/u to GeV/u, however, cooling the ion beams to a momentum spread $\Delta p/p$ below 10^{-4} using electron cooling suffers from the fact that the energy transfer in Coulomb collisions between electrons and ions depends on their relative velocity $v_{\rm rel}$ as[1] $dE_{\rm ecool}/ds \propto v_{\rm rel}^{-2}$ [3]. At highly relativistic energies, efficient electron cool-

ing thus requires the use of electron beams of several hundred mA and energies of several MeV [4, 5] - therefore electron cooling has been proposed only for the FAIR New Experimental Storage Ring (NESR) and High Energy Storage Ring (HESR) and not for the Schwerionen-Synchrotron SIS100/300.

With laser cooling of ion beams in storage rings, the situation changes drastically. For increasing beam energy the laser cooling force increases both due to the relativistic Doppler shift as well as the properties of the atomic cooling transition of the ion of interest [6, 7]. Unlike to the laser cooling of ions in traps, which is limited to a few ion species due to the lack of suitable laser sources, tuning the laser frequency ω_l in the laboratory frame to the cooling transition frequency in the rest frame $\omega_r = (1+\beta)\gamma\omega_l, \beta = v_{\rm beam}/c$ via a change in beam energy γ provides for laser cooling of a variety of Li-like and Na-like ions using a single laser system [8]. The saturation of cooling transitions exploiting this relativistic Doppler frequency shift allows for precision spectroscopy for a wide range of wavelengths up to the x-ray spectrum [7, 9, 10].

CHALLENGES OF LASER COOLING ION BEAMS AT RELATIVISTIC ENERGIES

Besides the benefits of laser cooling ion beams, recent results [1, 11] indicate several challenges when considering laser cooling to be applied at future high energy storage rings[2]:

1. Laser cooling is efficient only along the direction of the propagation of the laser beam.

2. Thus, additional coupling between the longitudinal motion of the ions along the beam axis to their transverse betatron motion is required to efficiently cool all three degrees of freedom of the ion motion.

3. At previous beam times at ESR, initial moderate electron cooling of the beam was required to yield enough fluorescence for optical detection, although laser cooling proved to be efficient.

---

[*] m.bussmann@fzd.de

[1] Here and in the following text we omit the energy dependence of the Coulomb logarithm for the sake of simplicity.

[2] For an in-depth discussion see [8]

4. The momentum acceptance of the laser force is usually orders of magnitude smaller than the initial momentum spread of the ion beam.

5. At high ion currents intra-beam scattering counteracts the laser force and close encounters of ions in the beam can force ions outside the momentum acceptance of the laser force.

6. Consequently, at previous experiments, the laser force could only counteract intra-beam scattering when the ion beam current was about 10 μA.

7. At low currents, when the transition to the space charge dominated regime occurs, all ion charge based detection devices such as the beam profile monitor or the Schottky pickup electrode are close to or reach their resolution limit.

Although items 1 and 2 have been addressed both in experiment [12, 13] and in theoretical works [14], up to now, no feasible approach to three-dimensional laser cooling at highly relativistic energies has been demonstrated. In the following, we will thus focus on the experimental approach towards all-optical beam cooling and characterization planned for the upcoming ESR beam time, thereby concentrating on items 3 to 7 in detail.

INCREASING THE MOMENTUM ACCEPTANCE OF THE LASER FORCE AND COUNTERACTING INTRA-BEAM SCATTERING

At previous ESR beam times, detuning the bunching frequency relative to the frequency of a single-mode single-frequency Ar+ ion laser [15] has been used to subsequently address all ions in the phase space of the bucket [9]. This required a stepwise change of the bunching frequency which at each step caused a replacement of the bucket center in momentum space relative to the mean momentum of the ions and thus lead to an oscillation of the ion bunch in the bucket [2].

We will follow a two-stage approach to enhance the laser force acceptance. Firstly, we will replace the Ar+ ion laser by a single-frequency diode laser system that will allow for scanning the laser frequency over a broad range without mode hopping.. The scanning range can be estimated by $\Delta f_1 = (c/\lambda_1) \times \Delta p_{\rm b}/p_{\rm b}$ and one finds with $\lambda_1 = 514$ nm $\Delta f_1 \approx 12$ GHz. Recently, a solid-state laser system has been introduced which is based on an external-cavity diode laser for which both the grating position and diode current are simultaneously controlled to avoid mode-hopping during frequency-tuning [16], providing several ten GHz of tuning range [16]. Such a system will require two times the doubling of the laser frequency via second harmonic generation. This in turn leads to a reduction in laser beam power. For laser cooling to become efficient one needs a laser intensity equal or greater than the saturation intensity $I_{\rm sat} = \pi ch\Gamma/(3\lambda_0^3) \approx 1.475$ Wcm^{-2} for the

$2S_{1/2} \rightarrow 2P_{3/2}$ transition in C^{3+} at $\lambda_0 = 154.81$ nm. This can be easily achieved using fiber amplifiers which deliver multi-Watt narrow line width output [17, 18].

In the future, simultaneous cooling of all ions in the bucket could be achieved using a pulsed laser system in addition to the continuous wave laser tuned close to the cooling transition [19]. The spectral bandwidth $\Delta\lambda_{\rm bw}$ of the pulsed laser should be large enough to address about half of the momentum acceptance of the bucket, giving $\Delta f_{\rm bw} = 6$ GHz. For a Gaussian-shaped pulse this results in a pulse duration of $\tau_1 = 0.44/\Delta f_{\rm bw} \approx 73$ ps. With a laser beam radius $r_{\rm beam} = 1$ mm matching the ion beam radius the required cooling power to saturate the cooling transition with a single-frequency laser can be estimated to[3] $P_{\rm sat} = I_{\rm sat} \times (\pi r_{\rm beam}^2) \approx 47$ mW. However, to saturate the transition with a pulsed laser, the spectral density of the pulse must be at least $I_{\rm sat}/\Gamma$. Since the spectral bandwidth of the pulse must be at least 6 GHz, we find a minimum pulse intensity of $I_{\rm pulse} = I_{\rm sat}\Delta f_{\rm bw}/\Gamma \approx 34$ Wcm^{-2}. This is a very moderate intensity. The required pulse intensity is in our case thus not determined by the atomic transition but instead by the requirement for doubling the center frequency of the pulse twice. For efficient second harmonic generation at a beam radius[4] of 100 μm we estimate a minimum pulse energy of about 50 μJ following [20] which gives a conversion efficiency of about 15 %, this means that for the second SHG stage focusing to a beam radius of 30 to 40 μm is required. At optimum, the repetition rate of the laser will be of the same order of the revolution frequency to achieve permanent temporal overlap. From these considerations the ideal laser system would be a 50 ps, 50 μJ laser system with a repetition rate of 1 MHz. This leads to a peak power of 1 MW and an average power of 50 W. Such systems are in reach of current technology [21], and, most importantly, can be built using fibre amplifier technology [22] as will be used for the scanning laser setup.

OPTIMIZING THE FLUORESCENCE DETECTION SYSTEM

At previous laser cooling beam times at ESR the only optical window which allowed for transmission of the fluorescence light at 154 nm was placed in a dedicated, field-free cavity section of the ring. Initial moderate electron cooling was required to detect fluorescence light using a VUV photomultiplier (VUV-PM) that was placed outside the beam tube with viewing direction perpendicular to the beam pipe. The fluorescence light was transmitted through a MgF$_2$ viewport attached to the experimental section of the ESR as shown in 1. High fluorescence yields can only be expected at small momentum spread when most ions in the beam can absorb the laser photons [23]. A variety of ef-

---

[3]Please note that this is the power required at a central wavelength of 257 nm.

[4]In the following the laser beam radius is decreased to lower the constraints on the pulsed laser system¡ without sacrificing cooling efficiency at low momentum spread.
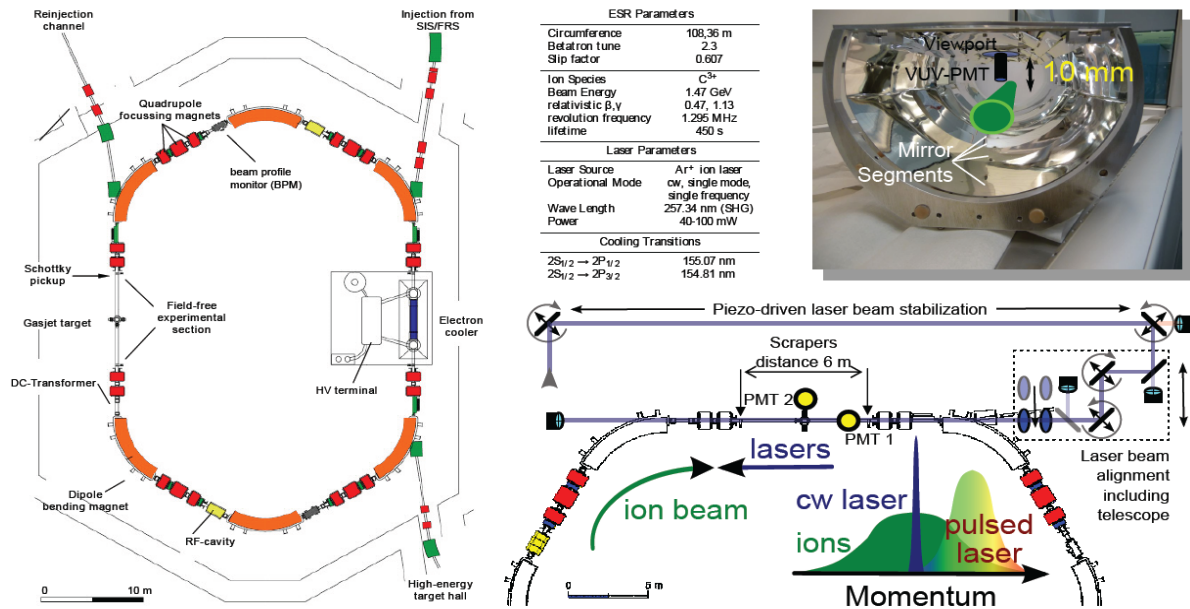
Figure 1: **Left:** Overview of the Experimental Storage Ring ESR at GSI. Ions are injected in the upper right part, revolving clockwise. The electron cooler system is found on the right, while the field-free experimental section is found opposite to the electron cooler on the left. Also shown are the two main diagnostic systems, the beam profile monitor (BPM, upper left) for measuring the beam width and the Schottky pickup electrode (field free section, left) for measuring the momentum spectrum of the ion beam. The parameters used for the 2004 and 2006 ESR experiments on laser cooling C^{3+} ion beams are listed in the table located on the right of the ESR overview. **Upper right:** Picture of the drift tube cavity after it has been dismantled in 2009. One can see the reflecting mirrors on the bottom of the tube opposite to the viewport windows, where a schematic drawing of a photomultiplier (PMT) that can be lowered into the tube using a motor-driven linear vacuum feedthrough has been added. The laser beam is indicated in green. **Lower right:** Detailed view of the field-free experimental section. A second PMT is added to the setup. Please note that the final position of the PMT has not yet been determined. Also shown are the scrapers that allow for the off-line positioning of the laser beam relative to the ion beam orbit. The laser beam line includes a newly developed Piezo-driven laser beam stabilization as well as a new beam alignment setup which will be used to optimize the overlap between laser beam and ion beam and to measure the ion beam width as explained in the text. A telescope can be put into the optical path, allowing for stronger focusing at small ion beam diameters. In the lower part, the overlap of the single-frequency laser and the broadband laser with the ion momentum distribution is indicated schematically.

fects can limit the fluorescence rate observed, most of them are related to the geometrical acceptance of the detector as well as relativistic effects, see [24] for an exhaustive discussion. These limitations can be overcome by installing an in-vacuum detector system which can be moved close to the ion beam.

A serious limitation to the fluorescence yield observed in the last two beam times was caused by using a single photomultiplier instead of at least two. With a single photomultiplier, only off-line alignment of ion beam and laser beam is possible, using the ESR beam scrapers as markers for the ion beam orbit to center the laser beam inside the beam tube. A second MgF_2 viewport will be added to the ESR beam line. This will make online beam overlap optimization possible by measuring the intensity of the fluorescence light detected at two different places along the region of overlap between ion and laser beam. In addition, we plan to add a motor-driven linear vacuum feedthrough

to the ESR beam tube. It will allow to move the photomultiplier close to the beam in order to increase the collection efficiency of the detector. Such a setup will require to add shielding to the detector that blocks stray light from the laser which otherwise would lead to unwanted background light seen by the detector.

OPTICAL DIAGNOSTIC OF LASER COOLED ION BEAM PROPERTIES

In the following we will discuss new diagnostic methods to determine the beam properties of laser-cooled ion beams. Since a high fluorescence yield is only to be expected at small momentum spread, the methods listed here cannot replace the standard beam diagnostics available at ESR. They should rather be seen as an extension of the existing diagnostic tools for precision measurements with ultra-cold ion beams interacting with laser light.

When considering laser cooled ion beams, very low momentum spreads severely limit the use of Schottky pickup measurements of the momentum spread. At ESR, the Schottky signal power decreases by orders of magnitude for momentum spreads below $\Delta p/p < 10^{-6}$, while the momentum resolution is essentially limited by the length of the Schottky pickup electrode to about $\Delta p/p < 10^{-6}$ [11]. The transition of the beam dynamics from the intra-beam scattering dominated regime to the space-charge dominated regime has, yet, only been observed for low beam currents on the order of 10 μA and below, since only at low ion currents the laser force was able to counteract intra-beam scattering. At such low beam currents however, the transverse beam size cannot be determined with great accuracy.

With the new diagnostics setup, beam width, bunch length and longitudinal momentum spread can be determined using all-optical techniques. Beam width measurements require precise alignment of laser and ion beam. With a new mirror setup using motor-driven translation stages, we will be able to not only align the laser beam using the fast, Piezo-driven beam stabilization system used in previous beam times, but can control the horizontal laser beam position on the complete interaction length, thus being able to scan over the horizontal ion beam profile. During a fast scan of the horizontal displacement $\Delta x_{\mathrm{radial}}$ of the laser beam relative to the ion beam the fluorescence signal rate $R_{\mathrm{fluo}}(\Delta x_{\mathrm{radial}}) \propto \exp(-\Delta x_{\mathrm{radial}}^2/2\sigma_{\mathrm{radial}}^2)$ can be recorded. From this measurement one can deduce the radial ion density beam profile and thus the beam width σ_{radial}.

The method of optical bunch length measurement used at the PALLAS storage ring [25] can be almost directly transferred to the ESR. At PALLAS, the bunching frequency is used as a trigger to start a multi-hit time-to-digital converter (TDC). The TTL-converted photomultiplier signal is used as a stop signal. The probability $P_{\mathrm{fluo}}(\tau_{\mathrm{delay}})$ to detect a photon after a certain delay time τ_{delay} is proportional to the axial local ion bunch density $n_{\mathrm{axial}}(z)$. By choosing the phase relative to the bunching frequency one can deduce the axial ion density $n_{\mathrm{axial}}(\beta \times \tau_{\mathrm{delay}}) \propto P_{\mathrm{fluo}}(\tau_{\mathrm{delay}})$.

Optical measurements of the momentum spread have already been tested in the 2004 ESR beam time [9]. A fast voltage ramp is applied to the drift tube electrodes, locally changing the ion momentum inside the drift tube. In order to scan the distribution, one finds for the scan range $U_{\mathrm{scan}} > \Delta p/p \times E_{\mathrm{beam}}/e$. For the C^{3+} beam energy of $E_{\mathrm{beam}} = 1.47$ GeV we find a fast voltage supply with a scanning range of -5 kV to +5 kV suitable for cold beams with $\Delta p/p \leq 7 \times 10^{-6}$. The time for one complete ramping cycle should be fast enough to not alter the velocity distribution by the laser force. The scanning time thus has to be smaller than the cooling time estimated by

$$\tau_{\mathrm{cool}} = \frac{\Delta p}{p} \times \frac{\beta\hbar\omega_r}{m_{C^{3+}}c^2} \times \frac{2}{\Gamma} \; .$$

When taking into account the length of the interaction region between laser and ion beam, incomplete saturation and the ratio of the Doppler-broadened saturation transition line width to the laser line width, cooling times of 20 ms could be reached at ESR. This means, the voltage ramp should be scanned in about 1 ms while simultaneously recording the fluorescence rate. With a scanning single-frequency laser system as described above, changing the laser frequency rather than changing the local beam velocity will give the same effect. Fast, mode-hop free scanning of the laser frequency on the order of 1 GHz/ms is in reach with modern laser systems, which would allow to resolve much larger momentum spreads.

As discussed, slow scanning of the laser frequency alters the velocity distribution. When the beam is very cold, this effect can be used to probe for the phase transition to the crystalline state as shown in [26]. At first, the laser frequency is detuned far from the cooling transition frequency and then constantly scanned towards the transition frequency. The fluorescence rate grows with decreasing detuning. If beam crystallization occurs, the fluorescence rate shortly decreases before sharply rising to its maximum. This short decrease is caused by a sudden decrease in ion velocity spread due to the crystallization. At small detuning, almost all ions are then out of resonance with the laser. With further reduction of the detuning all ions come in resonance with the laser, leading to a sharp increase in the fluorescence. For bunched beams, fluorescence peaks are observed for each harmonic h of the revolution frequency [27], but the general evolution of the fluorescence rate with detuning is universal and an unambiguous proof for beam crystallization.

Beam ordering can be detected without having to resort to optical methods [28, 29, 30], but long-range correlations as expected in beam crystallization cannot be easily resolved by Schottky measurements [31]. The situation changes if the interaction of ions with laser light is considered [32]. In the following we briefly discuss using the TDC setup mentioned before to measure the longitudinal ion dynamics. As in the case of the optical bunch length measurement, the TDC is used to record multiple photomultiplier signals. The temporal distribution of signals is then Fourier-transformed using a fast FFT algorithm to acquire the spectral distribution of the photomultiplier signals. This spectral distribution is directly related to the momentum distribution of the ions.

For the case of a crystalline coasting beam with N particles in which the particles are arranged in a string-like pattern, one would observe a strong peak in the Schottky spectrum at the $h = N$ harmonic of the revolution frequency. Even with very dilute beams of $N = 10^3$ ions this would lead to a frequency in the GHz range, which cannot be resolved

by the Schottky pickup electrode. Using a fast photo-multiplier with ns rise time and a TDC with sub-100 ps time resolution, high-frequency components in the signal spectrum up to GHz could be measured directly. Such a measurement would demand high fluorescence rates even at very low beam currents and thus does not seem feasible. However, due to the high temporal resolution of the optical detection, the transition to an ordered state could be resolved without ambiguity even for high ion beam currents. This is due to the fact that unlike in an ordinary Schottky measurement, the signal power does not decrease with decreasing momentum spread. In fact, the fluorescence signal is expected to rise at smaller momentum spread. The optical measurement of the momentum spectrum of the ion beam is thus complementary to the standard Schottky measurement.

SUMMARY

In the upcoming ESR beam time we will focus on replacing the scanning of the bunching frequency by scanning the laser frequency over a range of several GHz. Recent developments in diode laser technology make it possible to scan large frequency ranges without any mode hopping. Combining such a system with a pulsed broadband laser will enable us to address the complete phase space volume of the ion beam simultaneously without the need for initial electron cooling.

Optical detection systems to measure bunch width, length, momentum spread and momentum spectrum will complement the existing beam diagnostics at ESR and expand the resolution limits that have constrained precision measurements of the properties of ultracold ion beams in the past. With the fast scanning laser system an unambiguous determination of the phase transition from a liquid-like space-charge dominated beam to a crystalline state will be available.

REFERENCES

[1] U. Schramm, M. Bussmann, D. Habs et al., PAC05, Knoxville, May 2005, FOAD004, p. 403. http://www.JACoW.org

[2] M. Bussmann, U. Schramm, D. Habs et al, J. Phys. Conf. Ser. 88, 012043.

[3] G. Zwicknagel , C. Toepffer , P.-G. Reinhard, Phys. Rep. 309 (1999) 117.

[4] I. Augustin et al., Nucl. Instr. Meth. B 261(1-2) (2007) 1014.

[5] V. Litvinenko et al., PAC07, Albuquerque, June 2007, TUPMS076, p. 1347. http://www.JACoW.org

[6] U. Schramm , M. Bussmann , D. Habs Nucl. Instr. Meth. A 532(1-2) (2004), 348.

[7] H. Backe, Hyperfine Interactions 171(1-3) (2006), 93.

[8] U. Schramm, D. Habs, Progr. Part. Nucl. Phys. 53(2) 2004, 583.

[9] U. Schramm, M. Bussmann, D. Habs et al., Hyperfine Interactions 162(1) (2005), 181.

[10] U Schramm., M. Bussmann, D. Habs et al., STORI-2005, Bonn, May 2005, p. 324. http://www.fz-juelich.de/ikp/stori05/

[11] M. Bussmann, D. Habs, U. Schramm et al., COOL07, Bad Kreuznach, September 2007, FRM1C02, p. 226, http://www.JACoW.org.

[12] I. Lauer, U. Eisenbarth, M. Grieser et al., Phys. Rev. Lett. 81 (1998), 2052.

[13] U. Schramm, M. Bussmann, D. Habs et al., COOL05, Galena, September 2005, AIP Conf. Proc. 821 (2006), 509.

[14] H. Okamoto, A. M. Sessler, D. Möhl, Phys. Rev. Lett. 72(25) (1994), 3977.

[15] J. S. Hangst, J. S. Nielsen, O. Poulsen, P. Shi, J. P. Schiffer, Phys. Rev. Lett. 74(22) (1995), 4432.

[16] T. Führer, T. Walther, Opt. Lett. 33(4) (2008), 372.

[17] R. Nicolaescu, T. Walther, E. S. Fry, M. Muendel, Appl. Opt. 38(9) (1999), 1784.

[18] A. Seifert, M. Sinther, T. Walther, E. S. Fry, Appl. Opt. 45(30) (2006), 7908.

[19] S. N. Atutov, R. Calabrese, R. Grimm et al., Phys. Rev. Lett. 80(10) (1998), 2129.

[20] A. Borsutzky, R. Brnger, C. Huang, R. Wallenstein, Appl. Phys. B 52(1) (1991), 55.

[21] T. Omatsu, K. Nawata, M. Okida, K. Furuki, Opt. Express 15(15) (2007), 9123.

[22] A. Galvanauskas, M.-Y. Cheng, K.-C. Hou, K.-H. Liao, IEEE J. Sel. Top. Quant. Electr. 13(3) (2007), 559.

[23] U. Schramm, T. Schätz, M. Bussmann, D. Habs, J. Phys. B 36(3) (2008), 561.

[24] C. Novotny, PHD-Thesis, GSI Diss. 2009-06 March (2009), 82-97.

[25] U. Schramm, T. Schätz, M. Bussmann, D. Habs Physica Scripta T104 (2003), 189.

[26] T. Schätz, U. Schramm, D. Habs, Nature 412 (2001) 717.

[27] U. Schramm, T. Schätz, D. Habs, Phys. Rev. Lett. 87(18) (2001), 184801.

[28] M. Steck, K. Beckert, H. Eickhoff et al., Phys. Rev. Lett. 77 (1996) 3803.

[29] H. Danared, A. Källberg, K.-G. Rensfeld et al., Phys. Rev. Lett. 88 (2002), 174801.

[30] T. Shirai, M. Ikegami, S. Fujimoto, H. Souda, M. Tanabe, H. Tongu, A. Noda, K. Noda, T. Fujimoto, S. Iwata, S. Shibuya, A. Smirnov, I. Meshkov, H. Fadil, M. Grieser, Phys. Rev. Lett. 98(20) (2007), 204801.

[31] R.W. Hasse, COOL07, Bad Kreuznach, September 2007, THAP21, p. 213, http://www.JACoW.org.

[32] S. Atutov, V. Biancalana, R. Calabrese, T. Clauser, D. Diacono, V. Guidi, G. Lamanna, P. Lenisa, E. Mariotti, L. Moi, Nucl. Inst. Meth. A 430(1) (1999), 10.